Enhancement of magnetoelectric coupling in functionally graded ferroelectric and ferromagnetic bilayers

V. M. Petrov* and G. Srinivasan
Physics Department, Oakland University, Rochester, Michigan 48309, USA
(Received 12 July 2008; published 18 November 2008)

A model is presented for magnetoelectric (ME) effects in a functionally graded ferroelectric-ferromagnetic bilayer. A linear grading of the piezoelectric coefficient and permittivity in the ferroelectric and a similar grading of piezomagnetic coefficient in the ferromagnet are assumed. The ME coupling at low frequencies and at mechanical resonance due to bending oscillations have been estimated and applied to the specific case of bilayers of nickel zinc ferrite and lead zirconate titanate with the grading axis perpendicular to the sample plane. Both free-standing bilayers and bilayer on a substrate have been considered. The thickness dependence of piezomagnetic and piezoelectric coefficients leads to an additional flexural strain and the theory predicts an enhancement in the strength of ME coupling compared to homogeneous compositions. The enhancement in the case of a free-standing bilayer is on the order of 50% at low frequencies and at electromechanical resonance (EMR). For the case of a bilayer on a substrate, the low-frequency ME coefficient is maximum when the substrate and the bilayer are of equal thickness. The coupling weakens with increasing substrate thickness. With increasing substrate thickness, the ME coefficient at EMR is expected to show an initial rapid decrease, followed by an increase and a broad maximum. The resonance frequency is predicted to show a linear increase with increasing substrate thickness.

DOI: 10.1103/PhysRevB.78.184421 PACS number(s): 75.80.+q, 75.70.Cn, 77.65.Fs

I. INTRODUCTION

Materials that respond to multiple external stimuli with changes in physical and structural properties are known as multiferroics.[1,2] A subclass of such materials in which magnetic ordering and ferroelectricity occur simultaneously and allow coupling between the two are magnetoelectric (ME).[1–4] Most of the single-phase ME materials generally do not exhibit strong coupling at room temperature.[3] A relatively large ME coefficients, however, have been obtained in composites consisting of piezoelectric and magnetostrictive materials.[4] When a magnetic field is applied to the composites, the magnetostrictive phase induces a strain which in turn exerts stress on the piezoelectric phase, resulting in an electric polarization. Systems studied so far include barium titanate, lead zirconate titanate (PZT), or lead magnesium niobate-lead titanate (PMN-PT) for the piezoelectric phase and ferrites, manganites, transition metals or alloys for the magnetic phase.[5–10] Studies on such systems show a giant ME effect at low frequencies and orders of magnitude enhancement in the strength of coupling at electromechanical resonance (EMR) due to radial and bending modes for the composite.[11–13]

This work is on modeling of ME interactions in bilayers of functionally graded piezoelectric and magnetostrictive phases. Although the composites can mimic the functionality of a single-phase multiferroic, ME properties can be limited by interface inhomogeneities. The use of graded piezoelectric and magnetostrictive phases in a composite may provide a path for solving interface problems and enhancing the ME interactions. Here we model the ME interactions in a graded ferroic bilayer with linear variation in the piezoelectric and piezomagnetic coefficients.

Functionally graded ferroics are analogs of compositionally graded semiconductor structures that yielded electronic components such as junction diodes and transistors. Research into nonhomogeneous ferroics conversely, has primarily been confined to the study of bilayer and multilayer structures and has only recently been expanded to include polarization-graded ferroelectrics and magnetization-graded ferrites.[14–20] Thus, investigations of compositionally graded ferroics offer opportunities for discovering novel phenomena and devices. Graded ferroelectrics have been studied recently in some detail.[14–18,21,22] Compositional grading of ferroelectrics leads to important effects including grading of polarization resulting in a built-in potential and a vertically displaced hysteresis loop; enhanced electric-field tunability of dielectric permittivity; and a spontaneous strain and a strong dynamic electric-field response.[14,17,23] Previous modeling efforts on graded piezoelectrics include effects of an external bending or twisting stress, elastic waves, and thermally induced fracture and electromagnetoelastic behaviors.[24–30] The response of a graded piezoelectric-piezomagnetic material subjected to an external force was modeled by Sun *et al.*[31]

Studies on graded ferromagnets have been limited to magnetization-graded nickel zinc ferrite and hexagonal barium ferrites. Evidence for a built-in magnetization in Ni-Zn ferrite was obtained through ferromagnetic resonance and in barium hexaferrite through ac and dc susceptibility measurements.[19,20] Theoretical analysis of the systems in terms of its spatially dependent order parameter, i.e., the magnetization, yielded a value for the internal magnetic field consistent with experimental observations.

Here we model the ME interactions in a bilayer of ferroelectric phase with a linearly graded piezoelectric coefficient and permittivity and a ferromagnetic phase with linear grading of piezomagnetic coefficient. Studies indicate the feasibility of such grading of piezoelectric coefficient in PZT, PMN-PT, and bismuth strontium titanate (BST).[17,18,21,22,32] Similarly, linear grading of magnetization and piezomagnetic coefficient can be achieved in Ni-Zn or Ni-Co ferrites.[19,20] The present model focuses on a bilayer of graded nickel zinc

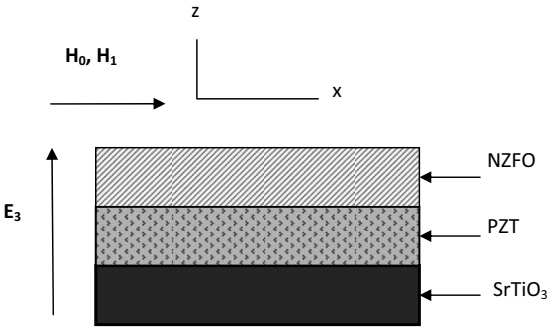

FIG. 1. A graded nickel zinc ferrite-lead zirconate titanate bilayer on $SrTiO_3$ substrate. The ferrite is assumed to have a grading of composition, leading to a linear variation in the piezomagnetic coefficient along its thickness. Similarly, the PZT layer is assumed to have linear variation in piezoelectric coefficient and dielectric constant along the z axis. The bias magnetic field H_0 and the ac magnetic field H_1 are parallel to x axis. The piezoelectric layer is poled along z and the ac electric field E_3 is measured across the bilayer.

ferrite (NZFO) and PZT with the grading axis perpendicular to its plane. Both free-standing bilayers and bilayers on a substrate have been considered. The principal aim is to estimate the ME coefficient at low frequencies and when the electrical subsystem shows mechanical resonance, at electromechanical resonance corresponding to acoustic modes. The ME voltage coefficients α_E have been estimated for field orientations that correspond to minimum demagnetizing fields and maximum α_E. The effect of substrate clamping has been described in terms of dependence of α_E on substrate volume. The thickness dependence of piezomagnetic and piezoelectric coefficients leads to an additional flexural strain and the theory predicts an enhancement in the strength of low-frequency ME coupling compared to homogeneous compositions. A similar increase in the ME coefficient is expected at radial and bending modes in the sample. The theory and application to NZFO-PZT bilayers are provided in Secs. II A–II D.

II. THEORY

We consider a bilayer of nickel zinc ferrite,$Ni_{1-x}Zn_xFe_2O_4$ (NZFO), and $Pb_{1-x}Zr_xTiO_3$ (PZT) as in Fig. 1. Although ferrites of homogeneous compositions are not piezomagnetic, one can achieve a pseudopiezomagnetic effect ($q=d\lambda/dH$, where λ is the magnetostriction) by subjecting the sample to a bias magnetic field H_0 and ac field H_1. Studies show that when Zn is substituted in nickel ferrite, the room temperature q varies linearly with increasing Zn concentration x for $x<0.4$.[33] Thus it is possible to achieve a linear grading in q with a compositionally graded NZFO. Similar grading of the piezoelectric coefficient d (and the dielectric constant ε) is possible by compositional grading of PZT.[34]

The analysis described here is based on the following equations for the strain, electric displacement and magnetic induction of piezoelectric, and magnetostrictive phases and the substrate:

$$
\begin{aligned}
{}^pS_i &= {}^ps_{ij}\,{}^pT_j + {}^pd_{ki}\,{}^pE_k;\\
{}^pD_k &= {}^pD_{ki}\,{}^pT_i + {}^p\varepsilon_{kn}\,{}^pE_n;\\
{}^mS_i &= {}^ms_{ij}\,{}^mT_j + {}^mq_{ki}\,{}^mH_k;\\
{}^mB_k &= {}^mq_{ki}\,{}^mT_i + {}^m\mu_{kn}\,{}^mH_n;\\
{}^sS_i &= {}^ss_{ij}\,{}^sT_j;
\end{aligned}
\tag{1}
$$

where S_i and T_j are strain and stress tensor components, E_k and D_k are the vector components of electric field and electric displacement, H_k and B_k are the vector components of magnetic field and magnetic induction, s_{ij}, q_{ki}, and d_{ki} are compliance, piezomagnetic, and piezoelectric coefficients, ε_{kn} is the permittivity matrix and μ_{kn} is the permeability matrix. The superscripts p, m, and s correspond to piezoelectric and piezomagnetic phases and substrate, respectively. Using the magnetostrictively graded ferrite and electrostrictively graded ferroelectric implies z dependence of piezomagnetic and piezoelectric coefficients q_{ki} and d_{ki}. We assume the symmetry of piezoelectric to be ∞m and the piezomagnetic to be cubic.

A. Low-frequency magnetoelectric effect

For finding the low-frequency ME voltage coefficient, we solve magnetostatic and elastostatic equations in NZFO, and elastostatic and electrostatic equations in PZT, taking into account boundary conditions. The longitudinal axial strains of each layer can be considered as linear functions of the vertical coordinate z_i to take into account the bending deformations of bilayer:[35]

$$
\begin{aligned}
{}^mS_1 &= {}^mS_{10} + z_m/R_1;\\
{}^pS_1 &= {}^pS_{10} + z_p/R_1;\\
{}^sS_1 &= {}^sS_{10} + z_s/R_1;\\
{}^mS_2 &= {}^mS_{20} + z_m/R_2;\\
{}^pS_2 &= {}^pS_{20} + z_p/R_2;\\
{}^sS_2 &= {}^sS_{20} + z_s/R_2;
\end{aligned}
\tag{2}
$$

where ${}^iS_{10}$ and ${}^iS_{20}$ are the centroidal strains along the x and y axes at $z_i=0$, R_1 and R_2 are the radii of curvature, and z_i is measured relative to center plane of i layer. It can be shown that the strains obey the following conditions:

$$
\begin{aligned}
{}^mS_{10} - {}^pS_{10} &= h_m/R_1,\\
{}^pS_{10} - {}^sS_{10} &= h_p/R_1,\\
{}^mS_{20} - {}^pS_{20} &= h_m/R_2,\\
{}^pS_{20} - {}^sS_{20} &= h_p/R_2.
\end{aligned}
\tag{3}
$$

We limit the analysis to field orientation in Fig. 1 in which the bias magnetic field H_0 and ac magnetic field H_1 are par-

allel to each other and the samples plane. The PZT is polarized along z and the ac electric field is measured perpendicular to the sample plane. The assumed field orientation provides minimum demagnetizing fields and maximum ME coefficient.[20] In this case, Eq. (2) can then be rewritten using Eqs. (3) and (1) as

$$
\begin{aligned}
&{}^{m}S_{10} + z_m/R_1 = {}^{m}s_{11}\,{}^{m}T_1 + {}^{m}s_{12}\,{}^{m}T_2 + {}^{m}q_{11}\,{}^{m}H_1\\
&{}^{m}S_{10} + (z_p - h_m)/R_1 = {}^{p}s_{11}\,{}^{p}T_1 + {}^{p}s_{12}\,{}^{p}T_2 + {}^{p}d_{31}\,{}^{p}E_3;\\
&{}^{m}S_{10} + (z_p - h_m - h_p)/R_1 = {}^{s}s_{11}\,{}^{s}T_1 + {}^{s}s_{12}\,{}^{s}T_2\\
&{}^{m}S_{20} + z_m/R_2 = {}^{m}s_{12}\,{}^{m}T_1 + {}^{m}s_{11}\,{}^{m}T_2 + {}^{m}q_{12}\,{}^{m}H_1\\
&{}^{m}S_{20} + (z_p - h_m)/R_2 = {}^{p}s_{12}\,{}^{p}T_1 + {}^{p}s_{11}\,{}^{p}T_2 + {}^{p}d_{31}\,{}^{p}E_3;\\
&{}^{m}S_{20} + (z_p - h_m - h_p)/R_2 = {}^{s}s_{12}\,{}^{s}T_1 + {}^{s}s_{11}\,{}^{s}T_2. \qquad (4)
\end{aligned}
$$

The axial forces in the three layers must add up to zero to preserve force equilibrium,

$$
\begin{aligned}
&{}^{m}F_1 + {}^{p}F_1 + {}^{s}F_1 = 0,\\
&{}^{m}F_2 + {}^{p}F_2 + {}^{s}F_2 = 0,
\end{aligned}
\qquad (5)
$$

where $F_{i1}=\int_{-{}^{i}t/2}^{{}^{i}t/2} {}^{i}T_1 dz_1$, $F_{i2}=\int_{-{}^{i}t/2}^{{}^{i}t/2} {}^{i}T_2 dz_1$, ${}^{m}t$, ${}^{p}t$, and ${}^{s}t$ are the thicknesses of piezomagnetic, piezoelectric, and substrate layers. Further, Eq. (4) should be solved for ${}^{i}T_j$ and substituted into Eq. (5). Using Eq. (5) and taking into account Eqs. (2) and (3) enables finding ${}^{m}S_{10}$ and ${}^{m}S_{20}$

$$
\begin{aligned}
{}^{m}S_{10} &= \frac{s_1}{t}\left[{}^{m}Y \int_{-{}^{m}t/2}^{{}^{m}t/2} {}^{m}q_{11}\,{}^{m}H_1 dz_1 \right.\\
&\left. + {}^{p}Y\left(\int_{-{}^{p}t/2}^{{}^{p}t/2} {}^{p}d_{31}\,{}^{p}E_3 dz_2 + \frac{{}^{p}t h_m}{R_1} \right) + {}^{s}t\,{}^{s}Y \frac{h_m + h_p}{R_1} \right],\\
{}^{m}S_{20} &= \frac{s_1}{t}\left[{}^{m}Y \int_{-{}^{m}t/2}^{{}^{m}t/2} {}^{m}q_{12}\,{}^{m}H_1 dz_{11} \right.\\
&\left. + {}^{p}Y\left(\int_{-{}^{p}t/2}^{{}^{p}t/2} {}^{p}d_{31}\,{}^{p}E_3 dz_2 + \frac{{}^{p}t h_m}{R_2} \right) + {}^{s}t\,{}^{s}Y \frac{h_m + h_p}{R_2} \right],
\end{aligned}
\qquad (6)
$$

where $s_1={}^{m}t({}^{m}t\,{}^{m}Y+{}^{p}t\,{}^{p}Y+{}^{s}t\,{}^{s}Y)^{-1}$, ${}^{m}t={}^{m}t+{}^{p}t$, ${}^{m}Y$, ${}^{p}Y$, and ${}^{s}Y$ are the modules of elasticity of piezomagnetic, piezoelectric components and substrate, correspondingly. To conserve moment, the rotating moments of axial forces in the three layers are counteracted by resultant bending moments $M_{\mathrm{m}j}$, $M_{\mathrm{p}j}$, and $M_{\mathrm{s}j}$, induced in piezomagnetic, piezoelectric, and substrate layers. That is,

$$
\begin{aligned}
&F_{m1}h_m + F_{p1}(h_m + h_p) = M_{m1} + M_{\mathrm{p}1} + M_{\mathrm{s}1},\\
&F_{m2}h_m + F_{p2}(h_m + h_p) = M_{m2} + M_{\mathrm{p}2} + M_{\mathrm{s}2},
\end{aligned}
\qquad (7)
$$

where $M_{i1}=\int_{-{}^{i}t/2}^{{}^{i}t/2} z_i\,{}^{i}T_1 dz_i$ and $M_{i2}=\int_{-{}^{i}t/2}^{{}^{i}t/2} z_i\,{}^{i}T_2 dz_i$.

Taking into account Eqs. (3), (4), and (6), the equilibrium condition [Eq. (7)] can be solved for R_1 and R_2. The expressions for R_1 and R_2 are not given here because of their inconvenience. The values of these radii of curvature can then be substituted into Eq. (6) to obtain the centroidal strains. Once the centroidal strains are determined, the axial stress ${}^{i}T_1$ can be found from Eq. (4). To obtain the expression for ME voltage coefficient, we use the open-circuit condition on the boundary

$$
D_3 = 0. \qquad (8)
$$

Since electric induction is divergence free and has only one component D_3, it is evident that D_3 is equal to zero for any z. In this case Eqs. (1) and (8) result in the expression for ME voltage coefficient

$$
\alpha_{E31} = \frac{E_3}{H_1} = -\int_{-{}^{p}t/2}^{{}^{p}t/2} \frac{{}^{p}d_{31}({}^{p}T_1 + {}^{p}T_2)}{t H_1\,{}^{p}\varepsilon_{33}} dz; \qquad (9)
$$

where E_3 and H_1 are the average electric field induced across the piezoelectric layer and applied ac magnetic field, ${}^{p}T_1$ and ${}^{p}T_2$ are determined by Eqs. (4) and (6).

B. Application to graded NZFO-PZT

As an example, numerical estimations of ME voltage coefficient are considered for a bilayer of NZFO-PZT. First we consider grading only in $Ni_{1-x}Zn_xFe_2O_4$ (NZFO) in which the piezomagnetic coefficient linearly varies with z:[33]

$$
\begin{aligned}
&{}^{m}q_{11} = {}^{m}q_{110}(1 + 2k z_1/{}^{m}t), \quad -{}^{m}t/2 \le z_1 \le {}^{m}t/2\\
&{}^{m}q_{12} = {}^{m}q_{120}(1 + 2k z_1/{}^{m}t),
\end{aligned}
\qquad (10)
$$

where ${}^{m}q_0$ is the average value of this parameter, and factor k specifies the grading strength and direction: $k>0$ and $k<0$ correspond to "positive" and "negative" magnetostriction grading, respectively. According to data on magnetostriction vs H of NZFO,[21] ${}^{m}q_{11}$ varies from -680 pm/A for pure nickel ferrite to -1156 pm/A for NZFO with $x=0.4$, with an average of -918 pm/V and a similar variation for ${}^{m}q_{12}$. In Eq. (10) we assume ${}^{m}q_{110}=-918$ pm/A and ${}^{m}q_{120}=169$ pm/A and $|k|=0.26$. In the calculations to follow, we use Eq. (10) for piezomagnetic coefficients of graded ferrites, and ${}^{m}q_{11}(z_1=0)={}^{m}q_{110}=-918$ pm/A for the homogeneous ferrite.

Similarly, the composition of PZT can be tailored to obtain linear grading of the piezoelectric coefficient and permittivity:[34]

$$
\begin{aligned}
&{}^{p}d_{31} = {}^{p}d_{310}(1 + 2k z_2/{}^{p}t), \quad -{}^{p}t/2 \le z_2 \le {}^{p}t/2\\
&{}^{p}\varepsilon_{33} = {}^{p}\varepsilon_{330}(1 + 2k z_2/{}^{p}t),
\end{aligned}
\qquad (11)
$$

with ${}^{p}d_{310}=-175$ pm/V, ${}^{p}\varepsilon_{330}/\varepsilon_0=1750$, and $|k|=0.35$.

Next we apply the theory to estimate the ME coefficients for (a) graded NZFO and homogeneous PZT, (b) homogeneous NZFO and graded PZT, and (c) grading of both NZFO and PZT. The material parameters used are listed in Table I. The ME coefficient vs PZT volume fraction V is shown in Fig. 2 for the case of homogeneous PZT and homogeneous, positively or negatively graded NZFO. Results of $\alpha_{E,31}$ vs V

TABLE I. Material parameters (compliance coefficient s, piezomagnetic coefficient q, permittivity ε and density ρ) for NZFO, PZT and $SrTiO_3$ used for theoretical estimates (Refs. 33 and 34).

Material	s_{11} (10^{-12} m^2/N)	Average q_{11} (10^{-12} m/A)	Average d_{31} (10^{-12} m/V)	Average d_{33} (10^{-12} m/V)	Average $\varepsilon_{33}/\varepsilon_0$	ρ (g/cm^3)
PZT	15.3		125	−400	1750	7.75
NZFO	6.5	−918				5.37
$SrTiO_3$	3.3					5.13

reveals a double maximum for all cases and is due to fact that the strain produced by the ferrite consists of two components: longitudinal and flexural. In the absence of a flexural strain the maximum ME coefficient occurs for $V=0.6$.[5] Since the flexural strain is of opposite sign relative to longitudinal strain and reaches its maximum value for $V=0.6$, the two types of strains combine to produce suppression of $\alpha_{E,31}$ at $V=0.6$ and a double maximum in the ME coefficient as in Fig. 2. Negative grading of NZFO leads to a maximum in $\alpha_{E,31}$ for low V whereas positive grading gives rise to a maximum for high V. The ME coefficient shows a 50% increase in $\alpha_{E,31}$ for negative grading of the piezomagnetic coefficient compared to the homogeneous case. Such dependence arises due to a decrease in the rotational moment of the ferrite layer for negative grading of q and an increase in the radius of curvature and longitudinal strain of PZT. It should be noted that the ME voltage according to Eq. (9) is determined by average longitudinal strains of the PZT layer.

The PZT volume fraction dependence of $\alpha_{E,31}$ is shown in Fig. 3 for the case of homogeneous NZFO and homogeneous or graded PZT. Simultaneous variations in ${}^{p}d_{31}$ and ${}^{p}\varepsilon_{33}$ leads to a constant value for the ratio ${}^{p}d_{31}/{}^{p}\varepsilon_{33}$ and the grading therefore cannot influence the ME voltage coefficient as defined by Eq. (9). But grading of the piezoelectric coefficient results in an additional variation in the volume average of the stress ${}^{p}T_1+{}^{p}T_2$. Thus z dependence of ${}^{p}d_{31}$ induces an additional flexural moment which gives rise to an increase in ME coefficient for positive grading and a decrease for negative grading, as seen in Fig. 3.

Figure 4 shows the anticipated effects of grading of both PZT and ferrite. Simultaneous grading leads to the highest ME voltage coefficient when the ferrite is negatively graded and PZT is positively graded.

Next we consider ME effects in bilayers on a substrate. Estimates are shown in Fig. 5 for homogeneous and graded bilayers with a thickness equal to the substrate thickness. It is seen that grading of NZFO and PZT leads to a general enhancement in the strength of ME coupling compared to the homogeneous composition. This could be attributed to the fact that the substrate yields a stress of the same sign as the axial stress of PZT. In a free-standing bilayer, however, half the PZT layer is under compression and the remaining under tension.

Figure 6 shows the variation in the ME coefficient as a function of the substrate thickness for a specific PZT volume fraction of 0.7. An increase in ${}^{s}t$ leads to a decrease in $\alpha_{E,31}$ due to clamping effects. The ME voltage coefficient for negatively graded NZFO and positively graded PZT exceeds that of the homogeneous case by 20%. This is explained by increase in the average stress of PZT due to additional rotating moments which enters Eq. (9) for the ME voltage coefficient.

C. Magnetoelectric effects at electromechanical resonance

In NZFO-PZT layered composites, a resonant enhancement of the ME coupling is expected when the ac magnetic

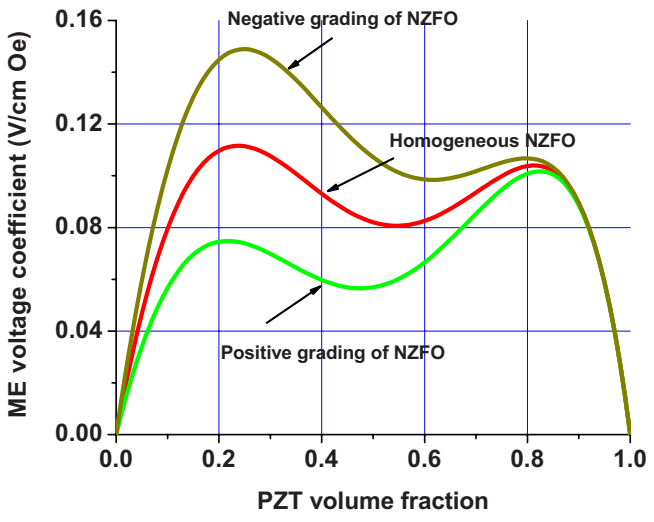

FIG. 2. (Color online) Low-frequency ME voltage coefficient as a function of PZT volume fraction for a free-standing PZT-NZFO bilayer. The results are for homogeneous PZT and homogeneous, positively, or negatively graded NZFO.

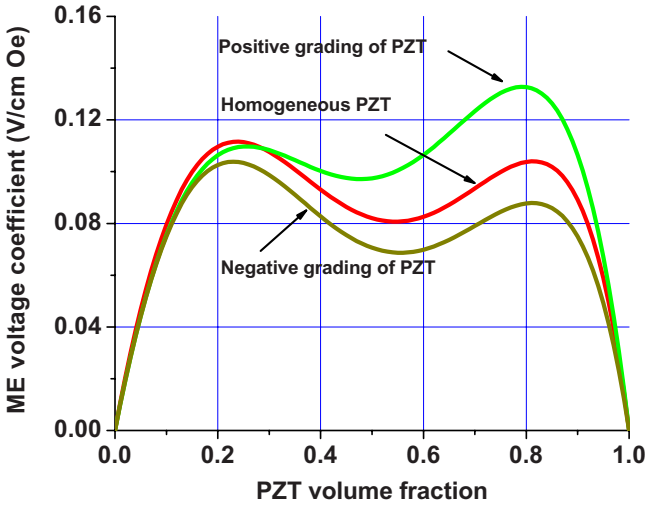

FIG. 3. (Color online) Similar results as in Fig. 2 but for bilayers of homogeneous NZFO and homogeneous, positively, or negatively graded PZT.

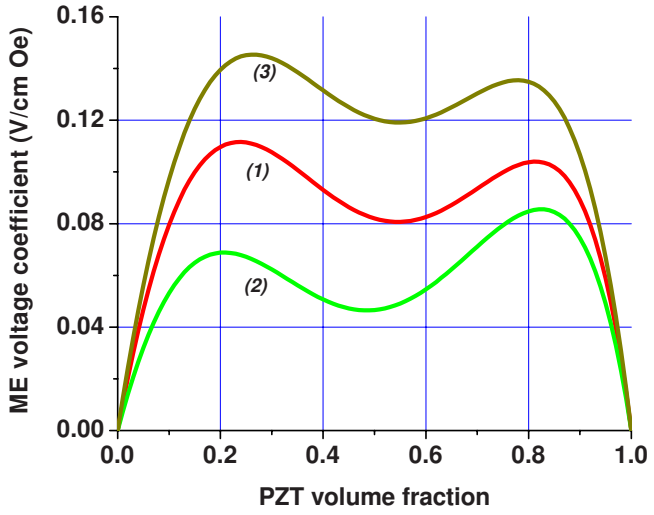

FIG. 4. (Color online) PZT volume fraction dependence of low-frequency ME voltage coefficient for bilayers of homogeneous NZFO-PZT (1), positively grading of NZFO and negatively graded PZT (2), and negative grading of NZFO and positive grading of PZT (3).

field is applied at the same frequency as the longitudinal, thickness, or bending modes of the structure. For nominal sample dimensions longitudinal or thickness acoustic modes occur at several hundred kilohertz whereas bending oscillations occur at a few kilohertz.[4,7] Studies reveal a much higher enhancement in the strength of ME coupling for bending than for other modes. Here we focus only on modeling resonance ME effects due to bending oscillations in bilayers. A similar treatment could be extended to cover other modes.

Magnetoelectric coupling is considered at bending modes in a graded NZFO-PZT bilayer on a substrate as in Fig. 1. The thickness of the sample is assumed to be small compared to other dimensions. Moreover, the bilayer width is assumed to be small compared to its length. The fields and the polarization are the same as in Fig. 1. In that case, we can consider only one component of strain and stress tensors in the resonance region. The equation of bending motion of the composite has the form[36]

$$\nabla^2\nabla^2 w + \frac{\rho t}{D}\frac{\partial^2 w}{\partial t^2} = 0, \tag{12}$$

where $\nabla^2\nabla^2$ is biharmonic operator, w is the deflection (displacement in z direction), and t and ρ are thickness and average density of sample, respectively. For a bilayer on a substrate, $t={}^{p}t+{}^{m}t+{}^{s}t$, $\rho=({}^{p}\rho\,{}^{p}t+{}^{m}\rho\,{}^{m}t+{}^{s}\rho\,{}^{s}t)/t$, where ${}^{p}\rho$, ${}^{m}\rho$, and ${}^{s}\rho$ are densities of piezoelectric and piezomagnetic layers and substrate, respectively, and D is cylindrical stiffness.

Equation (12) relates to the middle plane, each point of which moves only in z direction. The position of middle plane is generally defined by equating the total force acting on the sample cross section in x direction to zero. This force is determined by stresses in bilayer components and substrate, which can be expressed in terms of strains from Eq. (1). Due to the fact that magnetic induction is divergence free, $\frac{\partial {}^{m}B_1}{\partial x}$ equals zero for transverse fields' orientation. For simplifying computations, the constitutive equations in Eq. (1) for magnetostrictive phase should be replaced in this case by

$$\begin{aligned} {}^{m}S_i &= {}^{m}s_{ij}^{B}\,{}^{m}T_j + {}^{m}g_{ki}\,{}^{m}B_k; \\ {}^{m}H_k &= -{}^{m}g_{ki}\,{}^{m}T_i + {}^{m}\beta_{ki}\,{}^{m}B_n; \end{aligned} \tag{13}$$

where ${}^{m}s_{ij}^{B}$ is compliance at constant magnetic induction and ${}^{m}\beta_{ki}$ is reversible permeability at constant stress. The dis-

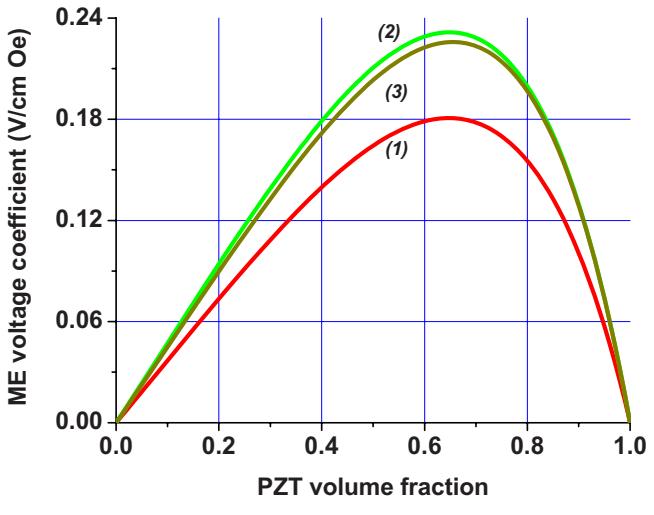

FIG. 5. (Color online) PZT volume fraction dependence of low-frequency ME voltage coefficient for a bilayer of NZFO and PZT on a $SrTiO_3$ substrate of equal thickness. Results are for homogeneous NZFO-PZT (1), positively graded NZFO and negatively graded PZT (2), negative grading of NZFO and positive grading of PZT (3).

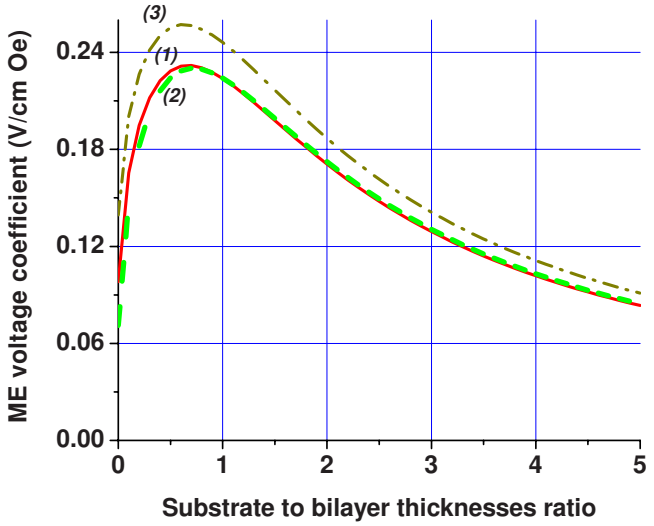

FIG. 6. (Color online) Substrate-to-bilayer thickness ratio dependence of ME voltage coefficient for a bilayer on a substrate. The estimates are for a PZT volume fraction of 0.7. Results are for homogeneous NZFO-PZT (1), positively graded NZFO and negative grading of PZT (2), and negative grading of NZFO and positively graded PZT (3).

tance of middle plane from NFO-PZT interface z_0 can be defined as follows:

$$z_0 = \frac{1}{2}\frac{{}^pY^p t^2 - {}^mY^m t^2 + {}^sY^s t^2 + 2{}^sY^p t^s t}{{}^pY^p t + {}^mY^m t + {}^sY^s t}. \quad (14)$$

Strains of both layers and substrate are related with the deflection of structure

$$ {}^pS_1 = -z\frac{\partial^2 w}{\partial x^2}, \quad z_0 - {}^pt < z < z_0,$$

$$ {}^mS_1 = -z\frac{\partial^2 w}{\partial x^2}, \quad z_0 < z < z_0 + {}^mt,$$

$$ {}^sS_1 = -z\frac{\partial^2 w}{\partial x^2}, \quad z_0 - {}^pt - {}^st < z < z_0 - {}^pt. \quad (15)$$

Cylindrical stiffness D of bilayer on a substrate can be calculated using the following expression:[35]

$$\frac{\partial M_1}{\partial x} = -D\frac{\partial^3 w}{\partial x^3}. \quad (16)$$

The moment of rotation M_1 is defined as

$$M_1 = \int_A zT_1 dz_1 \quad (17)$$

and A is the cross-sectional area of the sample normal to the x axis.

The general solution of Eq. (12) can be written for harmonic vibrations as

$$w(x) = C_1 \sinh(kx) + C_2 \cosh(kx) + C_3 \sin(kx) + C_4 \cos(kx), \quad (18)$$

where wave number k is defined by

$$k^4 = \frac{\omega^2 \rho t}{D}, \quad (19)$$

and ω is the frequency. The arbitrary constants C_1, C_2, C_3, and C_4 have to be found from boundary conditions at $x=0$ and $x=L$. Here L is length of the sample. As an example, we consider the plate with one end fixed and one end free. At fixed end, the deflection and derivative of deflection $\partial w/\partial x$ equal zero and at free end, the turning moment M_1 and transverse force V_1 equal zero

$$w = 0 \quad \text{and} \quad \partial w/\partial x = 0 \quad \text{at} \quad x = 0,$$

$$M_1 = 0 \quad \text{and} \quad V_1 = 0 \quad \text{at} \quad x = L, \quad (20)$$

where $V_1 = \frac{\partial M_1}{\partial x}$.

Substituting Eqs. (17) and (18) into Eq. (20) leads to a set of four equations. Solving this system for C_1, C_2, C_3, and C_4 enables obtaining the deflection from Eq. (18), strains from Eq. (15), and stresses from Eqs. (1) and (13). Once the stresses are determined, ME voltage coefficient can be then found using the open-circuit condition $\int_{z_0-{}^pt}^{z_0} {}^pD_3 dx = 0$. Using this condition and from Eq. (1), the ME voltage coefficient can be found as

$$\alpha_{E31} = \frac{E_3}{H_1} = -\int_{z_0-{}^pt}^{z_0} \frac{{}^pd_{31}{}^pT}{({}^pt + {}^mt){}^pH_1{}^p\varepsilon_{33}} dz, \quad (21)$$

where E_3 and H_1 are the average electric field induced across the sample and applied magnetic field. The energy losses are taken into account by substituting ω for complex frequency $\omega + i\omega'$ with $\omega'/\omega = 10^{-3}$.

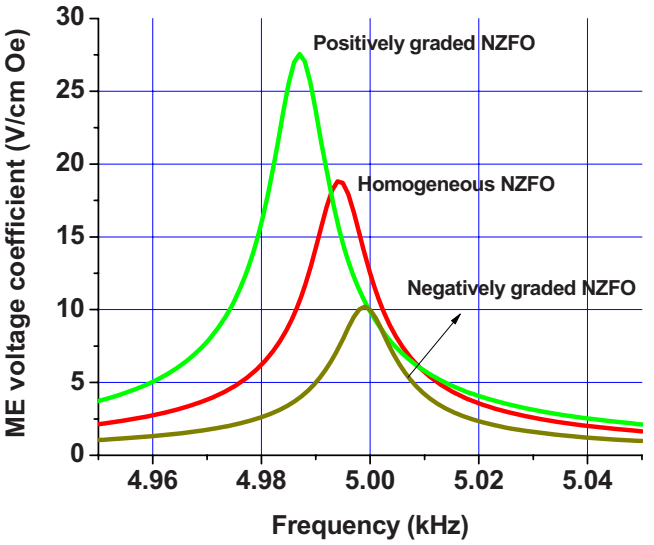

FIG. 7. (Color online) Frequency dependence of the ME voltage coefficient for a free-standing PZT-NZFO bilayer. The results are for homogeneous PZT and homogeneous, positively, or negatively graded NZFO. The PZT volume fraction is 0.3. The peak in ME coefficient occurs at resonance frequency for bending oscillations in the bilayer.

D. ME coupling at EMR in NZFO-PZT

Now we apply the model developed in Sec. II C to the case of NZFO-PZT. Figure 7 shows the frequency dependence of ME voltage coefficient for a free-standing bilayer of graded NZFO and homogeneous PZT with length 12 mm and thickness 2 mm and for PZT volume fraction $V=0.3$. The resonance in bending oscillations occurs at 5 kHz. The profile of $\alpha_{E,31}$ reveals a 2 order of magnitude increase in the maximum ME voltage coefficient compared to low-frequency coupling (Fig. 2). A small shift in the resonance frequency due to grading is predicted. In comparison to the homogeneous composition, a 50% increase in $\alpha_{E,31}$ for positive grading of the piezomagnetic coefficient and a 50% decrease for negative grading are expected. Such dependence can be attributed to an increase in the rotating moment of the ferrite layer for positive grading and a corresponding increase in the longitudinal strain of PZT, resulting in an increase in the ME voltage.

A similar $\alpha_{E,31}$ vs f for bilayers of homogeneous NZFO and graded PZT is shown in Fig. 8. It is seen that grading of PZT essentially leads to a shift of the resonance frequency,

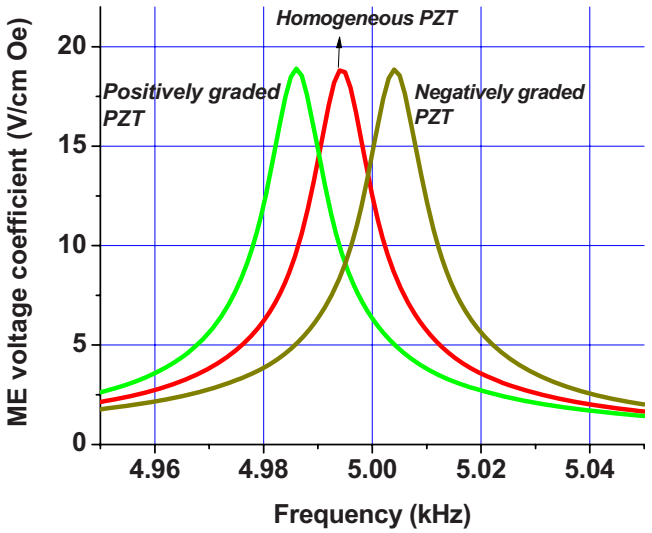

FIG. 8. (Color online) Frequency dependence as in Fig. 7 for free-standing bilayers of homogeneous NZFO and homogeneous, positively, or negatively graded PZT. The PZT volume fraction is 0.3.

but no changes in the magnitude of $\alpha_{E,31}$. The constant magnitude for $\alpha_{E,31}$ is expected from Eq. (21). The ratio d_{31}/ε_{33} and the ME voltage remain constant since both piezoelectric coupling and dielectric constant have the same grading related variation. Based on the results in Figs. 8 and 9, one expects maximum ME voltage coefficient for positive grading of both components.

Figure 9 shows the estimated resonance value of ME coefficient for homogeneous and graded bilayers. The results are shown as a function of PZT volume V. The maximum in the voltage occurs for a volume fraction of around 0.6, with the positive grading resulting in the highest voltage for all V values. The ME voltage coefficient vanishes at $V \approx 0.05$ for a

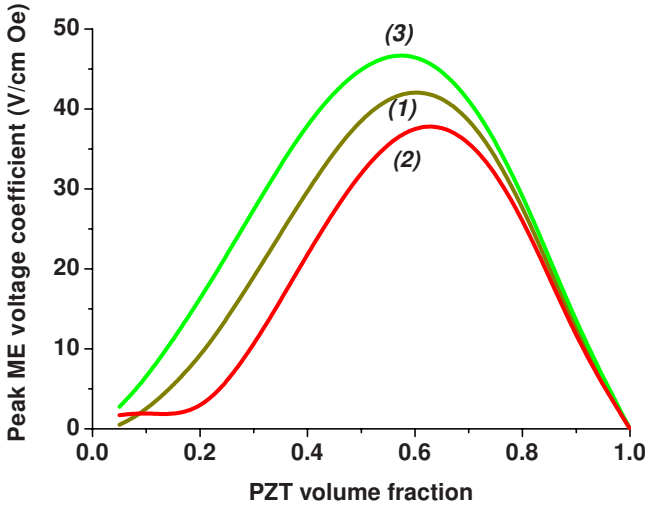

FIG. 9. (Color online) PZT volume fraction dependence of peak ME voltage coefficient at resonance for bending modes. The results are for free-standing bilayer of homogeneous components (1), negative grading of both PZT and NZFO (2), and positive grading of both PZT and NZFO (3).

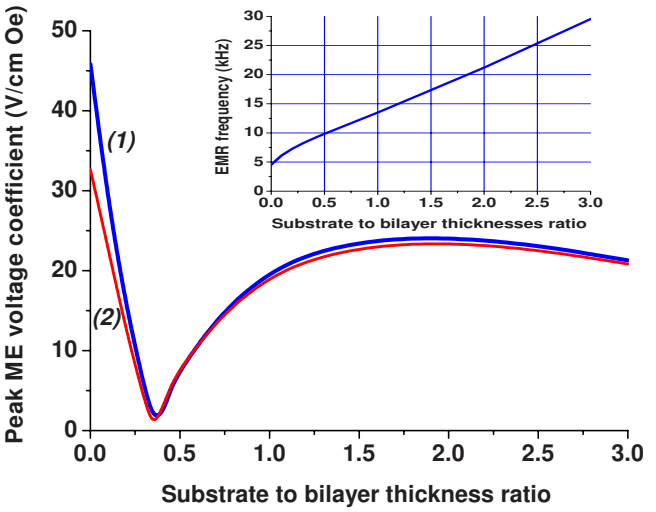

FIG. 10. (Color online) Substrate to bilayer thicknesses ratio dependence of peak-ME voltage coefficient at EMR for bilayer with positive grading of both PZT and NZFO (1), and negatively grading of both PZT and NZFO (2) for PZT volume fraction 0.5. The inset shows thickness ratio dependence of resonance frequency for bending modes for positive grading of both PZT and NZFO.

bilayer of homogeneous components and is related to near zero average axial stress in PZT due to lateral and flexural deformations.

Finally, we consider the resonance ME effects in a bilayer on a substrate. The estimated variation in the resonance frequency and ME voltage at resonance due to bending modes are shown in Fig. 10. The results are for either positive or negative grading of both PZT and NZFO. Estimates on the resonance frequency show a linear increase with increasing substrate thickness. The ME voltage initially shows a rapid decrease with increasing substrate thickness until it reaches a minimum at ${}^{s}t/({}^{p}t+{}^{m}t) \approx 0.3$. The minimum corresponds to sign reversal in the average axial stress of the PZT layer. The voltage coefficient then increases to show a broad maximum centered at a thickness ratio of 1.8. The influence of grading slowly decreases with increasing substrate thickness.

III. CONCLUSION

The ME interactions in a functionally graded ferroelectric-ferromagnetic bilayer is discussed. A linear variation in piezoelectric coefficient and permittivity is assumed in the ferroelectric and a linear grading of piezomagnetic coefficient for the ferromagnet. The model is applied to a representative case of nickel zinc ferrite and PZT. A free-standing bilayer and a substrate mounted structure are considered. The strength of ME coupling has been estimated for low frequencies and for bending oscillations. The ME voltage coefficients α_E have been estimated for magnetic-field orientations that correspond to minimum demagnetizing fields and maximum α_E. The effect of substrate clamping has been described in terms of dependence of α_E on substrate volume.

The grading related thickness dependence of piezomagnetic and/or piezoelectric coefficients leads to an additional

flexural strain and the theory predicts an enhancement in the strength of low-frequency ME coupling compared to homogeneous compositions. A similar increase in the ME coefficient has been predicted for mechanical resonance in bending modes in the sample. In graded bilayers the ME voltage coefficient is expected to increase by 50% at low frequencies and at mechanical resonance. For a graded bilayer on a substrate, the low-frequency ME voltage coefficient is higher by 20% in comparison to the homogeneous bilayer. The maximum ME coupling occurs for equal thickness of bilayer and substrate. At EMR, the ME voltage shows a sharp drop with increasing substrate thickness and then increase to show a broad maximum.

The theory presented here is likely to interest experimentalists in pursuing investigations on graded bilayers of PZT, lead magnesium niobate-lead titanate, or barium strontium titanate for the ferroelectric phase and nickel zinc ferrite, nickel cobalt ferrite, or transition metals or alloys for the ferromagnetic phase.

ACKNOWLEDGMENT

The work was supported by grants from the National Science Foundation, the Army Research Office and the Office of Naval Research.

*Permanent address: Novgorod State University, Veliky Novgorod, Russia.

[1] Hans Schmid, in *Introduction to Complex Mediums for Optics and Electromagnetics*, edited by W. S. Weiglhofer and A. Lakhtakia (SPIE, Bellingham, WA, 2003), pp. 167–195.
[2] N. A. Spaldin and M. Fiebig, Science **309**, 391 (2005).
[3] M. Fiebig, J. Phys. D **38**, R123 (2005).
[4] Ce-Wen Nan, M. I. Bichurin, S. Dong, D. Viehland, and G. Srinivasan, J. Appl. Phys. **103**, 031101 (2008).
[5] G. Srinivasan, E. T. Rasmussen, J. Gallegos, R. Srinivasan, Yu. I. Bokhan, and V. M. Laletin, Phys. Rev. B **64**, 214408 (2001).
[6] B. W. Li, Y. Shen, Z. X. Yue, and C. W. Nan, J. Appl. Phys. **99**, 123909 (2006).
[7] J. Zhai, Z. Xing, S. Dong, J. Li, and D. Viehland, Appl. Phys. Lett. **88**, 062510 (2006).
[8] K. Mori and M. Wuttig, Appl. Phys. Lett. **81**, 100 (2002).
[9] S. Sahoo, S. Polisetty, C.-G. Duan, S. S. Jaswal, E. Y. Tsymbal, and C. Binek, Phys. Rev. B **76**, 092108 (2007).
[10] R. Bergs, R. A. Islam, M. Vickers, H. Stephanou, and S. Priya, J. Appl. Phys. **101**, 024108 (2007).
[11] M. I. Bichurin, D. A. Filippov, V. M. Petrov, V. M. Laletsin, N. Paddubnaya, and G. Srinivasan, Phys. Rev. B **68**, 132408 (2003).
[12] Z. Xing, S. Dong, J. Zhai, Li Yan, J. Li, and D. Viehland, Appl. Phys. Lett. **89**, 112911 (2006).
[13] Zhan Shi, Jing Ma, Yuanhua Lin, and Ce-Wen Nan, J. Appl. Phys. **101**, 043902 (2007).
[14] Z. G. Ban, S. P. Alpay, and J. V. Mantese, Phys. Rev. B **67**, 184104 (2003).
[15] J. V. Mantese, N. W. Schubring, A. L. Micheli, M. P. Thomson, R. Naik, and G. W. Auner, Appl. Phys. Lett. **81**, 1068 (2002).
[16] S. Zhong, S. P. Alpay, and J. V. Mantese, Appl. Phys. Lett. **87**, 102902 (2005).
[17] S. Zhong, S. P. Alpay, M. W. Cole, E. Ngo, S. Hirsch, and J. D. Demaree, Appl. Phys. Lett. **90**, 092901 (2007).
[18] M. W. Cole, C. V. Weiss, E. Ngo, S. Hirsch, L. A. Coryell, and S. P. Alpay, Appl. Phys. Lett. **92**, 182906 (2008).
[19] J. V. Mantese, A. L. Micheli, N. W. Schubring, R. W. Hayes, G. Srinivasan, and S. P. Alpay, Appl. Phys. Lett. **87**, 082503 (2005).
[20] C. Sudakar, R. Naik, G. Lawes, J. V. Mantese, A. L. Micheli, G. Srinivasan, and S. P. Alpay, Appl. Phys. Lett. **90**, 062502 (2007).
[21] L. Jiankang and Y. Xi, Integr. Ferroelectr. **76**, 117 (2005).
[22] B. Vilquin, G. Poullain, R. Bouregba, and H. Murray, Thin Solid Films **436**, 157 (2003).
[23] S. Zhong, Z.-G. Ban, S. P. Alpay, and J. V. Mantese, Appl. Phys. Lett. **89**, 142913 (2006).
[24] X. Wang, E. Pan, J. D. Albrecht, and W. J. Feng, Compos. Struct. **87**, 206 (2009).
[25] J. Chen, Z. Liu, and Z. Zou, Arch. Appl. Mech. **72**, 686 (2003).
[26] E. Pan and F. Han, Int. J. Eng. Sci. **43**, 321 (2005).
[27] C. W. Lim and L. H. He, Int. J. Mech. Sci. **43**, 2479 (2001).
[28] Z. Zhong and E. T. Shang, Int. J. Solids Struct. **40**, 5335 (2003).
[29] X. Han and G. R. Liu, Smart Mater. Struct. **12**, 962 (2003).
[30] S. Ueda, J. Therm. Stresses **27**, 291 (2004).
[31] J.-L. Sun, Z.-G. Zhou, and B. Wang, Acta Mech. **176**, 45 (2005).
[32] R. Ranjith, A. Laha, and S. B. Krupanidhi, Appl. Phys. Lett. **86**, 092902 (2005).
[33] *Magnetic and Other Properties of Oxides*, Landolt-Bornstein, New Series, Group III, Vol. 4, Pt. B, edited by K.-H. Hellwege and A. M. Springer (Springer-Verlag, New York, 1970).
[34] *Piezoelectric Ceramics Materials Properties* (American Piezo Ceramics, Mackeyville, PA, 1998), Document Code 13085.
[35] S. Timoshenko and S. Woinowsky-Krieger, *Theory of Plates and Shells* (Mc Graw-Hill, New York, 1959).
[36] J. E. Ashton and J. M. Whitney, *Theory of Laminated Plates* (Technomic, Stamford, 1970).